J|A|C|S ARTICLES

Published on Web 03/29/2010

Molecular Wheels as Nanoporous Materials: Differing Modes of Gas Diffusion through Ga_{10} and Ga_{18} Wheels Probed by Hyperpolarized ^{129}Xe NMR Spectroscopy

Chi-Yuan Cheng, Theocharis C. Stamatatos, George Christou, and Clifford R. Bowers*

Department of Chemistry, University of Florida, Gainesville, Florida 32606-7200

Received October 6, 2009; E-mail: russ@ufl.edu

Abstract: The study of crystals of molecular wheels as nanoporous materials is reported. Hyperpolarized ^{129}Xe NMR spectroscopy has been used to characterize the mode of molecular diffusion and Xe interactions within the supramolecular nanochannels formed upon crystallization of the molecular wheels $[Ga_{10}(OMe)_{20}(O_2CMe)_{10}]$ and $[Ga_{18}(pd)_{12}(pdH)_{12}(O_2CMe)_6(NO_3)_6](NO_3)_6$. In agreement with expectations based on the collision diameter of the Xe atom relative to the differing internal diameters of the two types of gallium wheels, single-file diffusion occurs in the Ga_{10} channels, whereas in the Ga_{18} system the data are consistent with normal, Fickian diffusion. Information about the electronic environment inside the channels was probed by the Xe chemical shift. The interaction of the gas with the channel walls is found to be substantially stronger than the interaction in organic nanotubes and zeolites. The results establish the ability of crystals of molecular wheel compounds to function as a new class of porous nanotubular materials, and ones of a known and variable diameter, for studying the channel diameter dependence of molecular exchange and unidirectional diffusion on the micrometer length scale.

Introduction

Supramolecular chemistry offers virtually unlimited possibilities for fabrication of nanostructured materials. The power of the bottom-up approach is that the desired functionality of the final self-assembled structures is preprogrammed into the molecular building-blocks.[1−6] Crystalline supramolecular materials often exhibit porosity on various length scales, and porosity is of course central to many vital technologies, including gas storage, separations, and catalysis. The pores in a supramolecular assembly are defined by the interactions and interconnections between subunits, or by an ordered registration of a structural element inherent to the individual molecule. One-dimensional pores are particularly intriguing, because the tubular topology affords a high adsorption capacity with size selectivity and unidimensional diffusion properties. While X-ray structure determination can reveal the virtual porosity in a solid, adsorption analysis is necessary to establish the actual pore-space accessibility, guest−host interactions, and interconnectivity for a specified adsorbate. Furthermore, a fundamental understanding of the dynamics of gas exchange at the pore openings and diffusion within supramolecular channel networks is necessary to optimize performance in specific applications. Such studies require nanotube materials with well-defined, defect-free channels with tunable and monodisperse diameters.

Metal compounds with a cyclic structure that can be described as a 'molecular wheel' have been known for two decades since the initial reports of $[Cr_8F_8(O_2CBu^t)_{16}]$[7,8] and $[Fe_{10}(OMe)_{20}(O_2CCH_2Cl)_{10}]$.[9] Since then, a large family of such wheels has been reported, typically with a 'single-strand' topology with respect to the metal ions. Particularly beneficial synthetically has been the use of a central template whose size and nature determine the size (metal nuclearity) of the resulting wheel that forms around it. Examples include Fe_6 and Fe_8 wheels with a central Na^+ or Cs^+, respectively,[10] and the large family of homo- and heteronuclear wheels that contain organic amines or related templates in their central cavity.[11,12] However, such central templates prevent the crystal from exhibiting a well-defined nanoporous structure. In contrast, recent work replacing the MeO^- groups of $[Fe_{10}(OMe)_{20}(O_2CMe)_{10}]$, and the corresponding $[Ga_{10}(OMe)_{20}(O_2CMe)_{10}]$ (abbreviated Ga_{10}) analogue, with 1,3-propanediolate (pd^{2-}) has provided a nontemplate means to change the wheel size, giving new $[M_{18}(pd)_{12}(pdH)_{12}(O_2CMe)_6(NO_3)_6](NO_3)_6$

(1) Soldatov Dmitriy, V. In *Stimuli-Responsive Polymeric Films and Coatings*; American Chemical Society: Washington, DC, 2005; pp 214−231.
(2) Bein, T. In *Supramolecular Architecture*; American Chemical Society: Washington, DC, 1992; pp 1−7.
(3) Lehn, J. M. *Proc. Natl. Acad. Sci. U.S.A.* **2002**, *99*, 4763–4768.
(4) Hof, F.; Craig, S. L.; Nuckolls, C.; Rebek, J. *Angew. Chem., Int. Ed.* **2002**, *41*, 1488–1508.
(5) Tasiopoulos, A. J.; Vinslava, A.; Wernsdorfer, W.; Abboud, K. A.; Christou, G. *Angew. Chem., Int. Ed.* **2004**, *43*, 2117–2121.
(6) King, P.; Stamatatos, T. C.; Abboud, K. A.; Christou, G. *Angew. Chem., Int. Ed.* **2006**, *45*, 7379–7383.
(7) Gerbeleu, N. V.; Batsanov, A. S.; Timko, G. A.; Struchkov, I. T.; Indrichan, K. M.; Popovich, G. A. Patent SU No. 1299116, 1989.
(8) Gerbeleu, N. V.; Struchkov, I. T.; Timko, G. A.; Batsanov, A. S.; Indrichan, K. M.; Popovich, G. A. *Dokl. Akad. Nauk SSSR* **1990**, *313*, 1459–1462.
(9) Taft, K. L.; Lippard, S. J. *J. Am. Chem. Soc.* **1990**, *112*, 9629–9630.
(10) Saalfrank, R. W.; Bernt, I.; Uller, E.; Hampel, F. *Angew. Chem., Int. Ed. Engl.* **1997**, *36*, 2482–2485.
(11) Affronte, M.; Carretta, S.; Timco, G. A.; Winpenny, R. E. P. *Chem. Commun.* **2007**, 1789–1797.
(12) McInnes, E. J. L.; Piligkos, S.; Timco, G. A.; Winpenny, R. E. P. *Coord. Chem. Rev.* **2005**, *249*, 2577–2590.

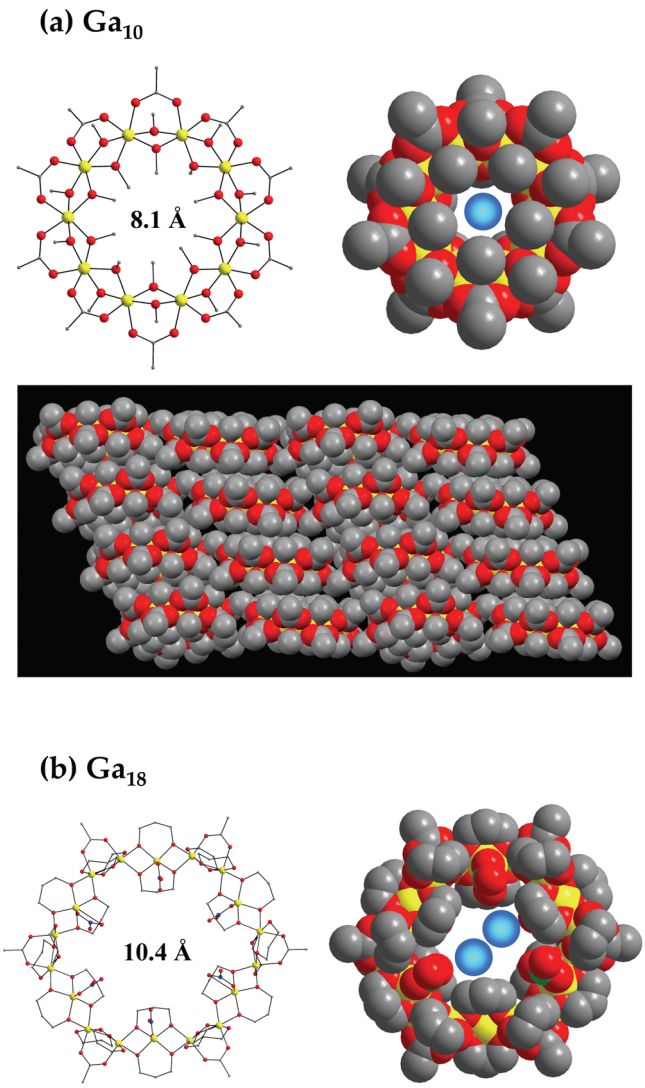

Figure 1. Ga molecular wheel structures. (a) Ga_{10}= $[Ga_{10}(OMe)_{20}(O_2CMe)_{10}]$. The lower panel shows a side-view of the packing arrangement of four adjacent channels. (b) Ga_{18}= $[Ga_{18}(pd)_{12}(pdH)_{12}(O_2CMe)_6(NO_3)_6](NO_3)_6$. Counterions have been omitted for clarity. Color code: Ga, yellow; O, red; N, green; C, gray; Xe, blue. Upon crystallization, the wheels stack to form nanotube structures with internal diameters of about 8.1 and 10.4 Å, respectively. In comparison, the Xe atom has a collision diameter of 4.4 Å. Thus, it is possible for two Xe atoms to pass within the Ga_{18} channels, but not in the Ga_{10} channels.

(M_{18}; M = Fe or Ga).[6] In fact, both the M_{10} and M_{18} wheels have empty central cavities (Figure 1), and in the crystal they thus stack to form supramolecular, nanotubular channels of a monodisperse diameter.

In this article, we illustrate for the first time how crystals of such molecular wheels can be used as nanoporous materials to control diffusive transport of a gas on micrometer length-scales. Using continuous-flow hyperpolarized ^{129}Xe NMR spectroscopy to probe the diffusion of Xe atoms within the channels, we show that by tuning the size of the Ga_x (x = 10, 18) wheel, a transition from single-file to normal one-dimensional diffusion can be induced, thus demonstrating the principle that long-range correlated motion within an extended solid can be directed at the molecular level. Our results illustrate that the ability to precisely control the channel diameter in molecular wheel nanotubes makes this class of materials particularly well-suited for testing the basic principles of molecular diffusion in one-dimension. Additionally, we probe the internal chemical and magnetic environments inside the channels of the crystals of gallium wheels via the ^{129}Xe NMR chemical shift and line shape.

Experimental Details

The synthesis of the Ga_{10} and Ga_{18} molecular wheels and their crystal structures can be found in the literature.[6] SEM images revealed needle-shaped Ga_{10} crystals with a distribution of lengths ranging from 500−600 μm. Approximately 40−50 mg of each polycrystalline samples was loosely packed into the NMR sample holder (described in ref 13), and evacuated in situ at room temperature to $\sim 10^{-5}$ mbar overnight prior to NMR measurements.

Hyperpolarized ^{129}Xe gas was generated in a continuous-flow Rb−Xe spin-exchange optical-pumping setup, as described elsewhere.[14] The gas mixture was circulated through the sample holder at a flow rate of ~100 mL/min. A total gas pressure of 4000 mbar was used in all experiments reported here. In the variable temperature studies, the gas mixture consisted of 2% Xe, 2% N_2, and 96% He. In the variable-pressure studies run at room temperature, the partial pressure of Xe was varied by mixing different ratios of Xe and He. All gases used were of natural isotopic abundance.

Hyperpolarized two-dimensional exchange (HP 2D-EXSY) spectra were acquired using the pulse sequences described in ref 15. During the repolarization delay of τ_1 = 2 s, the hyperpolarized Xe gas flows into the sample space and accumulates inside the channels. The 2D spectrum represents 64 × 1024 samples in the t_1 and t_2 dimensions, respectively. Eight transients were averaged for each t_1 increment. The spectral width is 38 kHz in both the t_1 and t_2 dimensions. In the interrupted-flow experiment, a settling time of τ_2 = 1 s was allowed following closing of the solenoid valve. The total acquisition time was about 25 min. The t_1 dimension was zero-filled to 1024 points, and a 300 Hz Gaussian line-broadening was applied in both time dimensions prior to the Fourier transformation.

The HP tracer exchange NMR pulse sequence[16] begins with the application of a frequency-selective saturation pulse train to initially destroy the Xe polarization in the nanotube phase. This is followed by a period τ, during which the spin polarization recovers due to exchange with the polarized gas phase. A nonselective $\pi/2$ pulse is applied to acquire the spectrum. The tracer exchange experiments were conducted at several different Xe partial pressures ranging from 668 to 4000 mbar. The NMR spectroscopy was performed in a 9.4 T Bruker Avance NMR spectrometer operating at 110.7 MHz. The $\pi/2$ pulse width was 4.5 μs. The ^{129}Xe chemical shifts are referenced to Xe gas. Spectra were acquired by signal averaging 16 or 32 transients for the Ga_{10} and Ga_{18} sample, respectively. A Gaussian line-broadening factor of 300 Hz was applied prior to Fourier transformation.

Results and Discussion

Single-file diffusion (SFD) is a universal phenomenon observed in systems of classical particles confined to one-dimensional (1D) channels where there is only a single translational degree of freedom.[16–23] As a consequence of the inability of the particles to pass one another in such channels, the mean square displacement along the channel axis becomes proportional to the square root of the observation time (τ), i.e. $\langle \Delta z(\tau)^2 \rangle = 2F(\theta)\tau^{1/2}$, where $F(\theta)$ is known as the single-file mobility and θ is the fractional channel occupancy. A hallmark

(13) Cheng, C. Y.; Bowers, C. R. *J. Am. Chem. Soc.* **2007**, *129*, 13997–14002.
(14) Zook, A. L.; Adhyaru, B. B.; Bowers, C. R. *J. Magn. Reson.* **2002**, *159*, 175–182.
(15) Cheng, C.-Y.; Pfielsticker, J.; Bowers, C. R. *J. Am. Chem. Soc.* **2008**, *130*, 2390–2391.
(16) Cheng, C. Y.; Bowers, C. R. *ChemPhysChem* **2007**, *8*, 2077–2081.
(17) Levitt, D. G. *Phys. Rev. A* **1973**, *8*, 3050.
(18) Kärger, J. *Phys. Rev. E* **1993**, *47*, 1427–1428.

of SFD is a drastic reduction in diffusion in comparison to normal Fickian diffusion (ND), wherein $\langle \Delta z(\tau)^2 \rangle = 2D\tau$, D being the diffusion constant. Much of the recent interest in molecular SFD in nanoporous materials derives from the potential to exploit it in vital processes, such as in catalysis and separations,[24,25] as demonstrated in recent molecular dynamics simulations.[26−28,52−53] However, experimental verification of the computer models has been lagging due to the scarcity of sufficiently ideal nanochannel−guest molecule systems, the inability to vary the channel size in most nanoporous materials, and the limitations of the available experimental techniques for probing molecular diffusion with sufficiently high time resolution over a wide range of observation times.

The Ga_{10} and Ga_{18} wheel structures, which consist of 10 and 18 Ga(III) atoms, stack to form supramolecular nanotubular assemblies with channel diameters of ∼8.1 Å and ∼10.4 Å, respectively.[6] With a collision diameter of 4.4 Å, it is possible for two Xe atoms to fit side-by-side in a Ga_{18} wheel, but not in the Ga_{10} wheel. On the basis of this simple geometrical consideration, completely different diffusion dynamics were anticipated for the two different wheels. The impossibility for Xe atoms to pass one another within the channels of the Ga_{10} nanotubes suggests that SFD should be observed in this system, while ND is possible only in Ga_{18} nanotubes.

The intrinsic properties of ^{129}Xe are well-suited for NMR spectroscopy characterization of nanoporous materials. The chemical shift is sensitive to pore size and shape, loading, channel orientation, and electronic environment.[29−34] Moreover, the availability of a $>10^4$-fold enhancement of the nuclear spin polarization (i.e., *hyperpolarization*) in ^{129}Xe[14,35] has led to the development of a new methodology for studying adsorption, exchange and diffusion in nanoporous materials.[13,15,16,22,36−42] In the recently introduced method of hyperpolarized (HP) ^{129}Xe NMR tracer exchange,[16,22] diffusion in nanotubes is monitored via atom exchange with the bulk hyperpolarized gas phase under conditions of sorption equilibrium. Because exchange requires diffusion to the channel openings, the time-dependence of the recovery of the adsorbed phase NMR signal following selective presaturation contains information about the time dependence of the mean square displacement. HP ^{129}Xe NMR tracer exchange was previously employed in the study single-file diffusion of Xe in the nanochannels of tris(*o*-phenylenedioxy)-cyclotrisphosphazene (TPP)[22] and L-alanyl-L-valine (AV).[16] Information was obtained on the diffusion time-scaling of the mean square displacement on time-scales ranging from 10^{-3} to 10^2 s. Continuous-flow hyperpolarized 2D exchange spectroscopy, which can be viewed in the present context as the extension of hyperpolarized tracer exchange NMR spectroscopy to two time dimensions, can be used to investigate pore space connectivity and molecular exchange between specific adsorption sites with the gas phase.[13,15,39,43−48] This method was recently applied to the kinetics of desorption for Xe atoms localized near the channel openings of AV nanotubes.[13,15]

Variable-Temperature and Variable-Pressure ^{129}Xe NMR Spectroscopy. At 25 °C, ^{129}Xe exhibits a symmetric NMR line shape centered at about 198 ppm in both the Ga_{10} and Ga_{18} nanotubes (see Figure 2). Such large Xe chemical shifts for physisorbed phases under ambient conditions are rarely seen in the literature. The interaction of the Xe atom with the channel wall appears to be particularly strong in the gallium wheel crystals. The line shape in each sample could be fit to a Lorentzian, yielding line widths of 8 and 14 ppm, respectively. In the Ga_{10} sample, the ratio of the integrals of the adsorbed- and gas-phase peaks remains constant as the Xe pressure is varied from 80 to 4000 mbar (at 25 °C), as shown in Figure 2. The same behavior was also found in the Ga_{18} sample. Thus, the loading of Xe in the channels is proportional to Xe pressure, consistent with the low loading regime of the gas adsorption isotherm.[29] The similarity of the chemical shifts in Ga_{10} and Ga_{18} nanotubes indicates that the morphology and chemical environment are each very similar in the two materials. By comparison, the ^{129}Xe chemical shifts reported (at any loading) in TPP and AV are much smaller (∼75−150 ppm range), even though the channels in these materials are substantially narrower

(19) Gupta, V.; Nivarthi, S. S.; McCormick, A. V.; Davis, H. T. *Chem. Phys. Lett.* **1995**, *247*, 596–600.
(20) Hahn, K.; Kärger, J.; Kukla, V. *Phys. Rev. Lett.* **1996**, *76*, 2762–2765.
(21) Wei, Q. H.; Bechinger, C.; Leiderer, P. *Science* **2000**, *287*, 625–627.
(22) Meersmann, T.; Logan, J. W.; Simonutti, R.; Caldarelli, S.; Comotti, A.; Sozzani, P.; Kaiser, L. G.; Pines, A. *J. Phys. Chem. A* **2000**, *104*, 11665–11670.
(23) Kärger, J.; Valiullin, R.; Vasenkov, S. *New J. Phys.* **2005**, *7*, 15.
(24) Caro, J.; Noack, M.; Kolsch, P.; Schafer, R. *Microporous Mesoporous Mater.* **2000**, *38*, 3–24.
(25) Liu, H.; Lei, G. D.; Sachtler, W. M. H. *Appl. Catal., A* **1996**, *137*, 167–177.
(26) Keffer, D. *Chem. Eng. J.* **1999**, *74*, 33–42.
(27) Adhangale, P.; Keffer, D. *Sep. Sci. Technol.* **2003**, *38*, 977–998.
(28) Brauer, P.; Brzank, A.; Clark, L. A.; Snurr, R. Q.; Kärger, J. *Adsorption Adsorption* **2006**, *12*, 417–422.
(29) Jameson, C. J.; de Dios, A. C. *J. Chem. Phys.* **2002**, *116*, 3805–3821.
(30) Moudrakovski, I. L.; Ratcliffe, C. I.; Ripmeester, J. A. *Zeolites: A Refined Tool for Designing Catalytic Sites: proceedings of the Internatinal Zeolite Sumposium, Quebec, Canada, October 15−20, 1995*; Bonneviot, L., Kaliaguine, S., Eds.; 1995; Vol. 97, pp 243−250.
(31) Moudrakovski, I.; Soldatov, D. V.; Ripmeester, J. A.; Sears, D. N.; Jameson, C. J. *Proc. Natl. Acad. Sci. U.S.A.* **2004**, *101*, 17924–17929.
(32) Soldatov, D. V.; Moudrakovski, I. L.; Ripmeester, J. A. *Angew. Chem., Int. Ed.* **2004**, *43*, 6308–6311.
(33) Soldatov, D. V.; Moudrakovski, I. L.; Grachev, E. V.; Ripmeester, J. A. *J. Am. Chem. Soc.* **2006**, *128*, 6737–6744.
(34) Clewett, C. F. M.; Morgan, S. W.; Saam, B.; Pietrass, T. *Phys. Rev. B* **2008**, *78*, 235402.
(35) Raftery, D.; Long, H.; Meersmann, T.; Grandinetti, P. J.; Reven, L.; Pines, A. *Phys. Rev. Lett.* **1991**, *66*, 584–587.
(36) Haake, M.; Pines, A.; Reimer, J. A.; Seydoux, R. *J. Am. Chem. Soc.* **1997**, *119*, 11711–11712.
(37) Seydoux, R.; Pines, A.; Haake, M.; Reimer, J. A. *J. Phys. Chem. B* **1999**, *103*, 4629–4637.
(38) Brunner, E.; Haake, M.; Kaiser, L.; Pines, A.; Reimer, J. A. *J. Magn. Reson.* **1999**, *138*, 155–159.
(39) Kneller, J. M.; Soto, R. J.; Surber, S. E.; Colomer, J. F.; Fonseca, A.; Nagy, J. B.; Van Tendeloo, G.; Pietrass, T. *J. Am. Chem. Soc.* **2000**, *122*, 10591–10597.
(40) Ruppert, K.; Brookeman, J. R.; Hagspiel, K. D.; Mugler, J. P. *Magn. Reson. Med.* **2000**, *44*, 349–357.
(41) Butler, J. P.; Mair, R. W.; Hoffmann, D.; Hrovat, M. I.; Rogers, R. A.; Topulos, G. P.; Walsworth, R. L.; Patz, S. *J. Phys.: Condens. Matter* **2002**, *14*, L297–L304.
(42) Pavlin, T.; Wang, R.; McGorty, R.; Rosen, M. S.; Cory, D. G.; Candela, D.; Mair, R. W.; Walsworth, R. L. *Appl. Magn. Reson.* **2007**, *32*, 93–112.
(43) Simonutti, R.; Bracco, S.; Comotti, A.; Mauri, M.; Sozzani, P. *Chem. Mater.* **2006**, *18*, 4651–4657.
(44) Sozzani, P.; Bracco, S.; Comotti, A.; Mauri, M.; Simonutti, R.; Valsesia, P. *Chem. Commun.* **2006**, 1921–1923.
(45) Moudrakovski, I. L.; Wang, L. Q.; Baumann, T.; Satcher, J. H.; Exarhos, G. J.; Ratcliffe, C. I.; Ripmeester, J. A. *J. Am. Chem. Soc.* **2004**, *126*, 5052–5053.
(46) Anala, S.; Pavlovskaya, G. E.; Pichumani, P.; Dieken, T. J.; Olsen, M. D.; Meersmann, T. *J. Am. Chem. Soc.* **2003**, *125*, 13298–13302.
(47) Knagge, K.; Smith, J. R.; Smith, L. J.; Buriak, J.; Raftery, D. *Solid State Nucl. Magn. Reson.* **2006**, *29*, 85–89.
(48) Comotti, A.; Bracco, S.; Valsesia, P.; Ferretti, L.; Sozzani, P. *J. Am. Chem. Soc.* **2007**, *129*, 8566–8576.

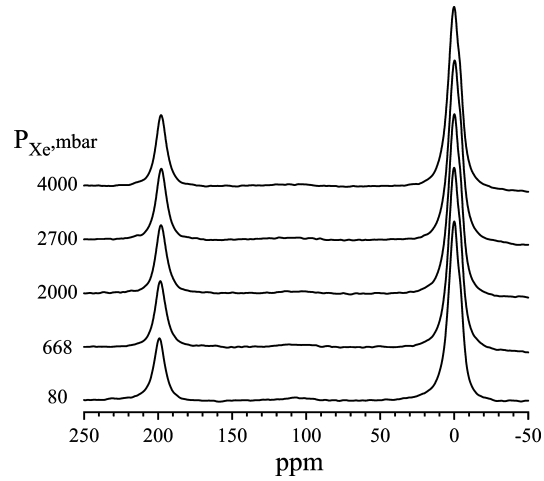

Figure 2. Continuous-flow hyperpolarized ^{129}Xe NMR spectra acquired in the Ga_{10} sample at the series of pressures indicated, at a constant temperature of 25 °C. Spectra were normalized to the gas peak, centered at 0 ppm. The total pressure is 4000 mbar.

(~4.7 Å and 5.1 Å, respectively).[31,49] Furthermore, TPP and AV yield a distinct chemical shift anisotropy (~20−30 ppm at low loading) which depends on the relative contributions of the Xe-channel and Xe−Xe interactions to the shielding tensor.[16,31,49] No such trend is observed in the gallium wheels, where the chemical shift and symmetric line shape of the adsorbed phase are found to be invariant to Xe pressure. These results suggest that for the range of experimental pressures studied here, the contribution of Xe−Xe interactions to the chemical shift remains smaller than the shift induced by interactions of Xe with the channel walls in the host material.

The adsorbed-phase ^{129}Xe chemical shifts in Ga_{10} and Ga_{18} nanotubes exhibit similar temperature dependences, as seen in Figure 3. The summary plot (Figure 4a) shows that the shifts increase in roughly linear fashion as the temperature decreases. Below 25 °C, the shift is smaller in the Ga_{18} sample by about 5−10 ppm, consistent with the larger channel diameter. The temperature dependences of the line widths in the two gallium wheels exhibit significant differences. As shown in Figure 4b, the full width half-maximum (fwhm) of the ^{129}Xe line in the Ga_{10} wheel increases monotonically with decreasing temperature, increasing sharply at −20 °C. The signal could not be detected at temperatures below −40 °C, where the fwhm exceeds 35 ppm. In the Ga_{18} sample, the line width decreases slightly as the temperature is reduced, passes through a minimum of about 9 ppm at −40 °C, and then abruptly increases. At −80 °C, the fwhm increases to 32 ppm, but the signal is still clearly detected. The abrupt increase in the fwhm indicates the temperature at which Xe becomes immobilized in the channels on the NMR time scale. Apparently, the diffusivity remains higher in the larger Ga_{18} channels than in the Ga_{10} channels at the same temperature.

In both samples, the gas-phase signal broadens and becomes increasingly asymmetric upon lowering the temperature. In the Ga_{10} sample, a distinct second peak emerges downfield of the gas peak, reaching a shift of about 5 ppm at −40 °C, with a discernible shoulder close to 10 ppm. In the Ga_{18} sample, the gas peak simply becomes asymmetric on the downfield side of the main gas peak. Signals in this low chemical shift range are

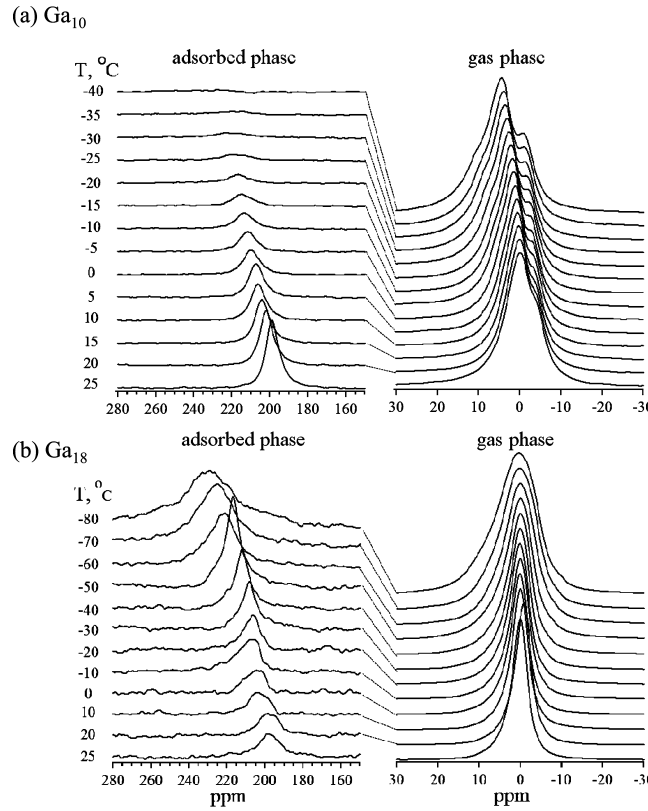

Figure 3. Continuous-flow hyperpolarized ^{129}Xe NMR spectra acquired in the (a) Ga_{10} and (b) Ga_{18} samples as a function of the sample temperature, as indicated. The gas mixture consisted of 2% Xe, 2% N_2, and 96% He (total pressure = 4000 mbar).

generally attributed to physisorbed xenon in fast exchange with the bulk gas phase.

Adsorption and Desorption at the Channel Openings. The individual processes of adsorption and desorption of Xe at the nanotube openings can be observed independently using continuous flow HP 2D-EXSY. The method has been employed in the characterization of porosity in a wide variety of microporous solids.[13,15,39,43–48] Recently, it was shown how the cross-peak signals in HP 2D-EXSY spectra, which provide direct evidence for exchange between the channels and surrounding gas phase, can be intensified by interruption of the gas flow.[15] Figure 5 provides a striking demonstration of this effect in the case of Ga_{10} wheel crystals. Using an exchange time of 250 ms, no gas peak signal along the diagonal (at 0 ppm, 0 ppm) can be detected, and only the slightest hint of a gas→channel exchange cross-peak can be seen above the noise. Only the diagonal peak corresponding to Xe atoms which remained inside the Ga_{10} channels throughout the mixing time is observed, because those atoms are not subject to purging by the flowing gas. At longer mixing times, no cross-peak or gas phase signals can be detected in continuous-flow mode. In comparison, when the flow of the hyperpolarized gas through the sample space is interrupted, intense gas-phase diagonal-peak and cross-peak signals appear, unequivocally demonstrating the processes of adsorption and desorption of Xe atoms at the channel openings of the nanotubes formed by the Ga_{10} molecular wheels.

Diffusion within Gallium Wheel Nanotubes. The HP NMR tracer exchange method utilizes a selective saturation-recovery pulse sequence. The spin polarization of ^{129}Xe atoms initially located within the channels is destroyed by a chemical-shift

(49) Sozzani, P.; Comotti, A.; Simonutti, R.; Meersmann, T.; Logan, J. W.; Pines, A. *Angew. Chem., Int. Ed.* **2000**, *39*, 2695–2698.

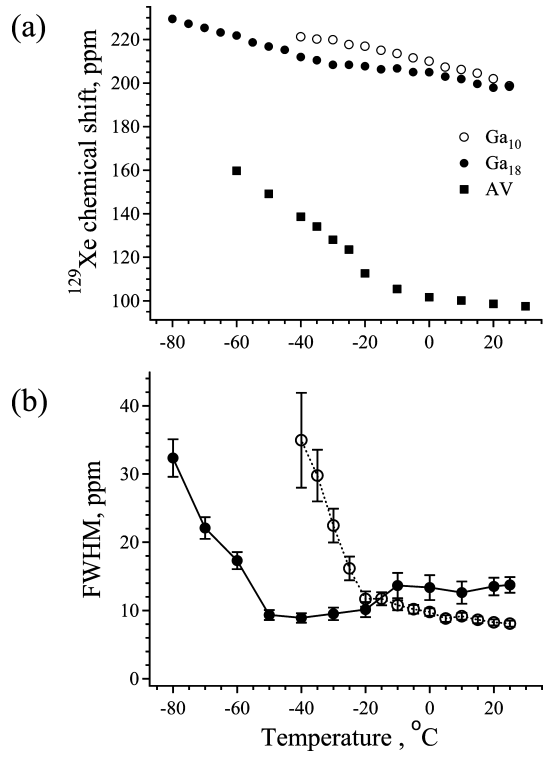

Figure 4. (a) Summary plot of the temperature dependences of the adsorbed-phase hyperpolarized ^{129}Xe chemical shifts in the Ga_{10} (open circles), Ga_{18} (filled circles), and AV nanotubes (filled squares). (b) Summary plot of the adsorbed-phase hyperpolarized ^{129}Xe peak full width half-maximum (fwhm) line widths in the Ga_{10} (open circles) and Ga_{18} (filled circles) samples.

selective pulse train. The recovery of the NMR signal of the adsorbed phase, $s_c(\tau)$, is subsequently recorded as a function of the postsaturation delay, τ.[16] By analogy with the conventional tracer exchange function,[50] we define the (normalized) NMR tracer exchange function as $\gamma_{nmr}(\tau) \equiv s_c(\tau)/s_c(\infty)$, where $s_c(\infty)$ is the steady-state continuous-flow HP NMR signal. In "long" channels, i.e. when the rms displacement on the time-scale of T_{1c} is much smaller than the channel length, the NMR tracer exchange expressions for SFD and ND are given by eq 1 and 2:

$$\gamma_{nmr}^{SFD}(\tau) = \frac{1}{\Gamma(1/4)T_{1c}^{1/4}} \int_0^\tau t^{-3/4}\, e^{-t/T_{1c}}\, dt \qquad (1)$$

$$\gamma_{nmr}^{ND}(\tau) = \frac{1}{(\pi T_{1c})} \int_0^\tau t^{-1/2}\, e^{-t/T_{1c}}\, dt \qquad (2)$$

In eq 1, Γ is the Euler gamma function. Nonlinear least-squares fitting to either γ_{nmr}^{SFD} or γ_{nmr}^{ND} involves only a single fitted parameter, T_{1c}. The degree of compliance to eqs 1 and 2 are compared to provide an assessment of the mode of diffusion.

The experimentally measured selective saturation-recovery traces in both gallium wheel samples, along with the least-squares fits to both eq 1 and 2, are shown in Figure 6. Clearly, at all four Xe partial pressures studied, the SFD model exhibits better overall compliance to the Ga_{10} data over the full range of τ values. This is confirmed by the R^2 values of the fits: $R^2 = 0.971$ (SFD) versus 0.964 (ND). The confidence intervals of

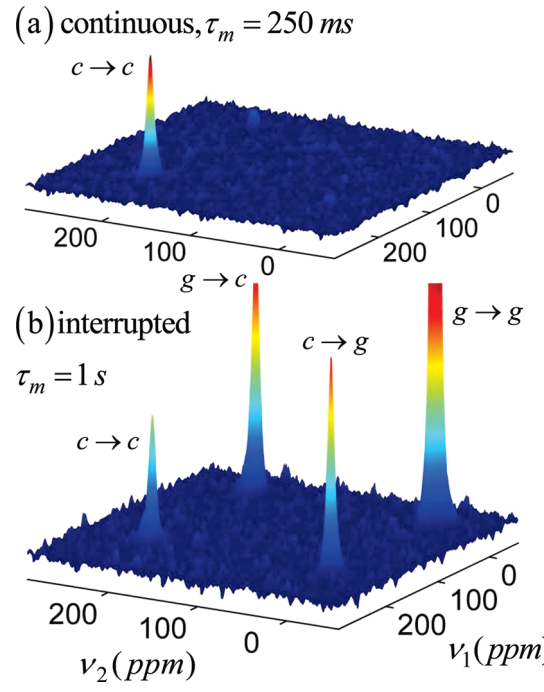

Figure 5. Hyperpolarized ^{129}Xe 2D exchange spectra in Ga_{10} nanotubes at 25 °C, acquired in (a) continuous flow mode, using a mixing time of 250 ms, and (b) interrupted flow mode, using a mixing time of 1s. The gas peak is truncated to facilitate comparison of the cross-peaks. Labeling of peaks is as follows: c→c (channel-to-channel) and g→g (gas-to-gas) diagonal peaks; c→g (channel-to-gas) and g→c (gas-to-channel) cross-peaks.

the fitted values for T_{1c} for all four pressures studied are overlapping, indicating that the spin−lattice relaxation is pressure independent over this range. The fits to γ_{nmr}^{SFD} for the Ga_{10} sample yielded $T_{1c} = 2.3 \pm 0.15$ s, averaged over the four runs. This is 2 orders of magnitude shorter than in AV at low loading.[16] In the Ga_{18} sample, eq 2 yielded the best fits at all three pressures studied (Figure Figure 6b), consistent with normal (i.e., Fickian) diffusion. Due to scatter in the data, the ability to distinguish the two diffusion modes is not as equivocal as in the Ga_{10} sample. Nevertheless, the inset of Figure 6b, which presents the data for recovery delays shorter than 300 ms, does exhibit slightly better compliance to the ND model. This is confirmed by the R^2 values of the fits: $R^2 = 0.944$ (SFD) versus 0.962 (ND). As in the Ga_{10} sample, T_{1c} in the Ga_{18} nanotubes is pressure independent over the range of pressures studied. We report a T_{1c} (averaged over all three pressure runs) of 82 ± 7 ms resulting from the fits to $\gamma_{nmr}^{ND}(\tau)$; nearly a factor of 30 shorter than in the Ga_{10} channels.

The ^{129}Xe T_{1c} relaxation times in Ga_{10} and Ga_{18} nanotubes extracted from the regression analysis are found to be insensitive to Xe pressure over a wide range, consistent with a spin−lattice relaxation mechanism dominated by Xe-channel interactions in the gallium wheel nanotubes. Notably, the spin−lattice relaxation times for ^{129}Xe in the gallium wheel samples are found to be several orders of magnitude shorter than in other diamagnetic single-file nanotube materials such as TPP and AV. Such a drastic reduction in T_{1c} may be indicative of the presence of paramagnetic impurities or defects. Assuming the same density of paramagnetic impurities in the gallium reagent used in the synthesis of the two wheels, the density of impurities per unit channel length would be expected to be greater by a factor of 9/5 in the larger Ga_{18} wheel nanotubes, resulting in a shorter T_{1c} in this sample. Qualitatively different translation dynamics

(50) Vasenkov, S.; Kärger, J. *Phys. Rev. E: Stat., Nonlinear Soft Matter Phys.* **2002**, *66*, 052601.

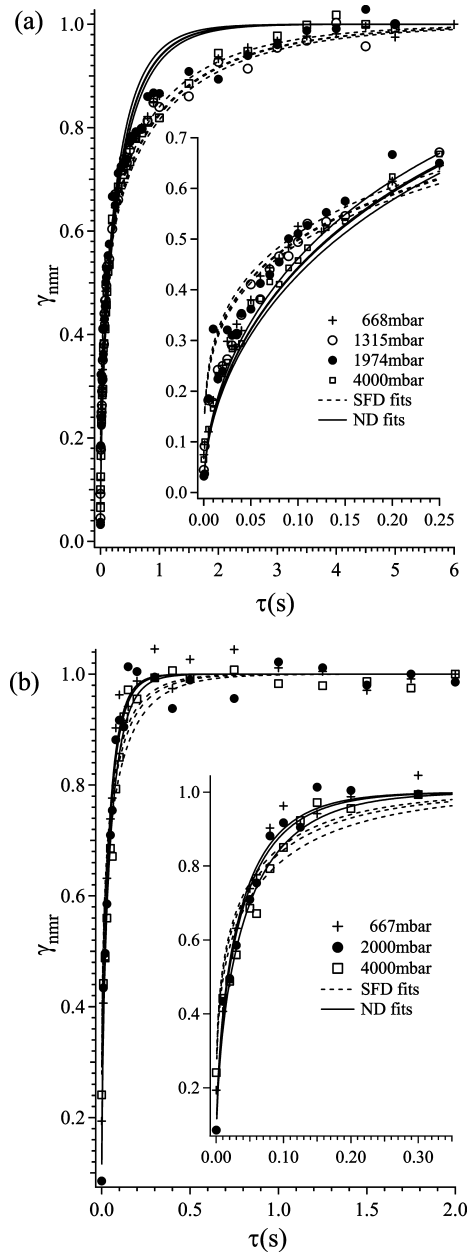

Figure 6. Continuous-flow hyperpolarized ^{129}Xe NMR tracer exchange data at 25 °C along with the results of nonlinear least-squares fits obtained in gallium wheel nantubes. (a) Selective saturation recovery traces in the Ga_{10} sample obtained with four different Xe/He mixtures ranging from 16.7% to 100% Xe, with a total pressure of 4000 mbar. Least-squares fits to eqs 1 and 2 are represented as dashed and solid lines, respectively. (b) Selective saturation recovery traces in the Ga_{18} sample at the three different Xe/He mixtures ranging from 16.7% to 100% Xe, with a total pressure of 4000 mbar. Least-squares fits to eqs 1 and 2 are represented as dashed and solid lines, respectively.

in the presence of the electron-spin bearing impurities could also play a role. According to the force free hard sphere model for the spectral density functions, the correlation time of fluctuations in the dipolar hyperfine interaction is given by $\tau_c = d^2/D$, where d is the distance of closest approach and D is the diffusivity. This mechanism could also account for the different temperature dependences of the line widths observed in the two different gallium wheel channels. Synthesis using Ga reagents of higher purity may reduce or effectively eliminate impurities such as iron, allowing the underlying Xe interactions with the channel walls and other Xe atoms to be unmasked.

Conclusions

The work described here represents proof-of-feasibility for the use of crystals of molecular wheels as supramolecular nanoporous materials for molecular diffusion studies. In addition, the availability of nontemplate methods for altering the wheel size (metal nuclearity), and thus the diameter of the vacant, central cavity, provides for such studies a family of molecular wheels of different but fixed and known central diameters. In the present work, we have employed only two, Ga_{10} and Ga_{18}, but others are available for related work in the future with a variety of cavity diameters up to ~19 Å as in the giant Mn_{84} wheel.[5]

The ^{129}Xe NMR spectroscopy data presented above indicate that the crystalline Ga_{10} and Ga_{18} nanochannels are open-ended and accessible to the gas phase, nominally devoid of blockages, and monodisperse in diameter. The variable Xe pressure dependence at 25 °C showed that the adsorbed phase signal scales in proportion to the gas pressure, indicating that the adsorption remains far from saturation for pressures up to 4000 mbar. At 25 °C the observed chemical shifts of ^{129}Xe within Ga_{10} and Ga_{18} nanotubes do not depend on Xe pressure, suggesting that the Xe-channel interactions dominate over the Xe−Xe interaction over the range of loadings tested. The chemical shifts in the Ga_{10} and Ga_{18} wheel nanotubes are found to be nearly the same, indicating similar Xe-channel wall interactions. The slightly smaller shift in the latter might be accounted for by the difference in the radius of curvature of the channels. The shifts are substantially greater than those reported in TPP, AV and zeolite channels. Another important difference is the absence of a chemical shift anisotropy in the gallium wheel materials. The anisotropy could be masked by one or more of the following: motional averaging effects, corrugation of the channels, dipolar hyperfine interactions, and inhomogeneous broadening.

Despite the similarity of the chemical environments presented to the Xe atom inside the channels of the Ga_{10} and Ga_{18} crystals, as evidenced by the chemical shift data, significant differences are observed in the spin−lattice relaxation times and mode of diffusion in the gallium wheel channels of different size. The nonlinear regression analysis of the HP NMR tracer exchange data reveals single-file diffusion in the Ga_{10} channels, while in the Ga_{18} system, the data are consistent with Fickian diffusion. The modes of diffusion observed in the two materials are consistent with expectations made on the basis of the known channel diameters relative to the size of the Xe atom. This illustrates that HP NMR tracer exchange is capable of distinguishing between normal one-dimensional Fickian diffusion and single-file diffusion of the confined atoms inside nanotubes with different internal diameters, and it represents the first use of hyperpolarized NMR spectroscopy to observe a transition from single-file to normal diffusion.

Finally, a new principle has been introduced: we have demonstrated that the diffusion time-scaling of a gas can be switched by a controlled size modification of a molecular building-block of a crystalline supramolecular assembly. Such channel-size-tunable materials are invaluable to validate the

predictions of recent numerical simulations which illustrate the potential to exploit single-file transport in separations and catalysis.

Acknowledgment. Acknowledgement is made to the Donors of the American Chemical Society Petroleum Research Fund for support of this project. G.C. thanks the National Science Foundation for support through Grants CHE-0414555 and CHE-0910472. We thank Yuying Wei for assistance with the SEM imaging. Construction of the spin-exchange optical pumping setup was supported by the In-House Research Program at the National High Magnetic Field Laboratory and the Division of Sponsored Research at the University of Florida.

Supporting Information Available: SEM images of $[Ga_{10}(OMe)_{20}(O_2CMe)_{10}]$ crystals. This material is available free of charge via the Internet at http://pubs.acs.org.

JA908327W

(51) Kärger, J.; Freude, D. *Chem. Eng. Technol.* **2002**, *25*, 769–778.
(52) Brzank, A.; Schutz, G. M.; Brauer, P.; Kärger, J. *Phys. Rev. E: Stat., Nonlinear Soft Matter Phys.* **2004**, *69*, 031102/1−031102/5.
(53) Sholl, D. S.; Fichthorn, K. A. *J. Chem. Phys.* **1997**, *107*, 4384–4389.